The EMBO Journal (2004) 23, 594–604 | © 2004 European Molecular Biology Organization | All Rights Reserved 0261-4189/04
www.embojournal.org

THE
EMBO
JOURNAL

The region 3′ to *Xist* mediates X chromosome counting and H3 Lys-4 dimethylation within the *Xist* gene

Céline Morey, Pablo Navarro, Emmanuel Debrand[1], Philip Avner, Claire Rougeulle and Philippe Clerc*

Génétique Moléculaire Murine, Institut Pasteur, rue du Docteur Roux, Paris, France

A counting process senses the X chromosome/autosome ratio and ensures that X chromosome inactivation (XCI) initiates in the female (XX) but not in the male (XY) mouse embryo. Counting is regulated by the X-inactivation centre, which contains the *Xist* gene. Deleting 65 kb 3′ to *Xist* in XO embryonic stem (ES) cells affects counting and results in inappropriate XCI upon differentiation. We show here that normal counting can be rescued in these deleted ES cells using cre/*lox*P re-insertion, and refine the location of elements controlling counting within a 20 kb bipartite domain. Furthermore, we show that the 65 kb deletion also leads to inappropriate XCI in XY differentiated ES cells, which excludes the involvement of sex-specific mechanisms in the initiation of XCI. At the chromatin level, we have found that the *Xist* gene corresponds to a peak of H3 Lys-4 dimethylation, which is dramatically and specifically affected by the deletion 3′ to *Xist*. Our results raise the possibility that H3 Lys-4 dimethylation within *Xist* may be functionally implicated in the counting process.

The EMBO Journal (2004) **23,** 594–604. doi:10.1038/sj.emboj.7600071; Published online 29 January 2004
Subject Categories: chromatin & transcription; RNA
Keywords: counting; histone dimethylation; X chromosome inactivation; *Xist*

Introduction

X chromosome inactivation (XCI), which occurs only in female (XX) and not in male (XY) embryos, ensures dosage compensation of X-linked genes between the sexes. The initial steps in XCI involve a 'counting process', which senses the X chromosomes/autosomes ratio and restricts XCI to female mouse embryos. Initiation of XCI in the embryo proper also includes the random choice of the active (Xa) and the inactive (Xi) Xs in each cell. The selected Xi becomes the target of a chromosome-wide mechanism of transcriptional silencing, which constitutes an exciting paradigm for epigenetic regulations and confirms interest in the molecular dissection of the X-inactivation centre (*Xic*), a locus on the X chromosome that contains the *Xist* gene and the elements involved in counting, choice and silencing.

The random form of XCI occurs around the time of implantation of the late female blastocyst, in the differentiating epiblast that derives from the inner cell mass (ICM) and that will give rise to the embryo proper. Mouse embryonic stem (ES) cells, which are derived from the ICM, constitute a useful *ex vivo* system for the study of random-XCI (Rastan *et al*, 1985; Panning and Jaenisch, 1996; Penny *et al*, 1996; Clerc and Avner, 1998). Female ES cells possess two active X chromosomes and recapitulate random XCI when induced to differentiate. Under the same differentiation conditions, male ES cells maintain their single X in the active state. *Xist* is expressed at very low levels from every X chromosome in both undifferentiated male and female ES cells. A transcript antisense to *Xist*, termed *Tsix* (Lee *et al*, 1999a), is initiated mainly 12 kb downstream of *Xist* at the *DXPas34* locus, and more weakly 28 kb downstream of *Xist* (Sado *et al*, 2001). *Tsix* is biallelically expressed in undifferentiated female ES cells and controlled in part by the *Xite* locus, a cluster of intergenic transcription start sites and *DNase*I hypersensitive sites (Ogawa and Lee, 2003). At the onset of XCI in differentiated female ES cells, *Tsix* is silenced on the elect inactive X chromosome, which becomes rapidly coated by *Xist* RNA (Panning *et al*, 1997; Sheardown *et al*, 1997) and transcriptionally silenced. In parallel, *Tsix* persists transiently on the Xa, where it represses *Xist* upregulation (Lee *et al*, 1999a, b; Luikenhuis *et al*, 2001; Morey *et al*, 2001; Sado *et al*, 2001; Stavropoulos *et al*, 2001).

Several covalent histone modifications are sequentially put in place following the accumulation of *Xist* RNA on the future Xi (H3 Lys-27 and Lys-9 hypermethylation and H3 Lys-4 hypomethylation, followed by hypoacetylation of both H3 and H4 (Heard *et al*, 2001; Mermoud *et al*, 2002; Plath *et al*, 2003; Silva *et al*, 2003)). These modifications are clearly major players in the establishment, spreading and maintenance of transcriptional silencing on the Xi. However, much less data are available on the role of histone modifications within the *Xic* in regulating the initiation of XCI. A H3 Lys-9 dimethylation hotspot spanning at least 150 kb upstream of the *Xist* gene is constitutively present in male and female ES cells (Heard *et al*, 2001). H3 Lys-9 dimethylation is generally correlated with regions of silent inactive chromatin (Rice and Allis, 2001). This has led to the proposal that the H3 Lys-9 dimethylation hotspot located 5′ to the *Xist* gene acts as a nucleation centre for the spreading of silencing along the Xi (Heard *et al*, 2001). Interestingly, a 120 kb region upstream to *Xist* has also been shown to present elevated levels of H4 acetylation in wild-type female ES cells but not in female cells bearing a heterozygous deletion of *Xist* (O'Neill *et al*, 1999). These data clearly point to the domain lying 5′ to *Xist* as a potential target for regulatory mechanisms, and calls for

*Corresponding author. Génétique Moléculaire Murine, Institut Pasteur, 25, rue du Docteur Roux, Paris 75015, France. Tel.: +33 1 45 68 86 25; Fax: +33 1 45 68 86 56; E-mail: pclerc@pasteur.fr
[1]Present address: Laboratory of Chromatin and Gene Expression, The Babraham Institute, Babraham, Cambridge CB2 4AT, UK

Received: 30 October 2003; accepted: 17 December 2003; Published online: 29 January 2004

analysis of other histone modifications within the *Xic* prior to and at the onset of the initiation of XCI.

The differential programming of XCI between male and female cells is poorly understood. It has been shown to depend on a counting process that senses the ratio of X chromosomes versus autosomes and ensures that every X is inactivated, with the exception of a single X per diploid set of autosomes (for a review, see Gartler and Riggs (1983)). Neither the mechanism of sensing nor the effector pathway acting downstream of it have been clearly identified. A simple model for counting would be that a 'blocking factor' binds to a specific region of the *Xic* referred to as the 'counting element' (Rastan *et al*, 1985). This blocking factor would be produced in a limiting quantity just sufficient to interact with a single counting element per diploid cell and to prevent the initiation of XCI in *cis*. A recent model additionally postulated the existence of a 'competence factor' that would be produced by cells bearing more than one X chromosome such as female cells (Lee *et al*, 1999b) and would be required to allow the initiation of XCI. Male/female differential XCI programming may also involve chromosome-wide epigenetic marks. Indeed, X-linked genes have been shown to present different levels of histone modifications in female ES cells as compared to male ES cells (O'Neill *et al*, 2003), while differential H4 acetylation of a region upstream of *Xist* has been reported (O'Neill *et al*, 1999). Another uncertainty related to counting concerns the moment in mouse embryonic development when the process occurs, either prior to the ICM stage or concurrently with epiblast differentiation.

The 'blocking factor' model for counting, which implies the existence of a mechanism capable of repressing the initiation of XCI, is supported by observations made on a 65 kb deletion targeted 3′ to *Xist* (Clerc and Avner, 1998). This deletion, which spans the *Tsix* antisense transcription, the *DXPas34* element and the *Xite* locus, was targeted to one of the Xs in an XX ES cell line and resulted in a complete skewing of random X inactivation in favour of the mutated X. Essentially XO ES cells carrying the targeted *Xic* were derived from the XX mutant ES cell line (D102 ES cell line) through selection of a spontaneous truncation of the unmutated X proximal to the *Hprt* locus. Interestingly, the targeted X in the XO ES cells (XLD ES cell line; Clerc and Avner, 1998) was able to efficiently initiate XCI upon differentiation, despite the fact that a single *Xic* is present in these cells. This result identifies a repressor associated with the 65 kb region lying 3′ to *Xist*, which mediates counting. This element is likely to be distinct from *Tsix* and *Xite* since individual mutations of these loci did not result in significant initiation of X inactivation in XY differentiated ES cells (Lee *et al*, 1999b; Luikenhuis *et al*, 2001; Sado *et al*, 2001, 2002; Ogawa and Lee, 2003). However, definitive elucidation of the phenotypic differences between the 65 kb deletion in XO ES cells as compared to the *Tsix* and *Xite* mutations in XY ES cells clearly requires testing of the 65 kb deletion in an XY ES cell line.

Here, we have investigated the counting process through both site-specific transgenesis using our original deleted XO ES cell line and *cre*/*lox*P deletion of an XY ES cell line. We show that inappropriate XCI induced by differentiation in the deleted XO ES cells is prevented by re-inserting a 37 kb DNA sequence spanning *Tsix* and *Xite*. This phenotypic complementation demonstrates that counting is not irreversibly established prior to ES cell differentiation, and refines the genomic span lying 3′ to *Xist* involved in counting. We also report that the 65 kb deletion results in efficient XCI upon differentiation of XY ES cells, similar to its effect in XO ES cells. The control exerted on the initiation of XCI by the region lying 3′ to *Xist* must therefore be able to override sex-specific marks on the X chromosome. As a further step towards characterizing the *Xic*, we have analysed the function of the region lying 3′ to *Xist* using chromatin immunoprecipitation (ChIP). We have found that the hotspot of H3 Lys-9 methylation lying 5′ to *Xist* is unaffected by the 65 kb deletion, suggesting that the hotspot does not act in the counting pathway downstream of the region 3′ to *Xist*. We have also analysed H3 Lys-4 dimethylation and found elevated levels of this histone modification within the *Xist* gene. We show that the deletion 3′ to *Xist*, which affects counting, has a dramatic and specific effect on H3 Lys-4 dimethylation within the *Xist* gene itself.

Results

Site-specific re-insertion of a 37 kb region 3′ to Xist in Δ65 XO ES cells re-establishes normal transcriptional and chromatin features

Using the *cre* site-specific recombinase, we have re-inserted into the deleted locus of the XLD ES cell line (Δ65 XO ES cells of 129/C3 H.Pgk1a background; Clerc and Avner, 1998) a 37 kb DNA sequence extending 3′ to *Xist* (Figure 1A). This region includes the terminal *Xist* exons, the *DXPas34* minisatellite (Debrand *et al*, 1999), the major and minor antisense start sites (Lee *et al*, 1999a; Sado *et al*, 2001), and the *Xite* locus (Ogawa and Lee, 2003). The genomic structure of the re-inserted ES cell clones was verified by Southern blot analysis (Figure 1B). Two independently complemented XLDp37 ES cell clones (XLDp37#5 and XLDp37#6) were systematically analysed. As both gave essentially similar results for all the experiments described in this paper, data for only a single clone are presented.

We first addressed the effect of the 37 kb re-insertion on *Xist* expression in undifferentiated ES cells. In the original 65-kb-deleted XLD ES cell line, the lack of antisense transcription was associated with a faint *Xist* pinpoint (Figure 1C, upper left panel) or with a diffusion of the *Xist* transcripts in the vicinity of their transcription site in about 15% of the nuclei ($n = 200$) (Figure 1C, down left panel). The XLD ES cell line also showed elevated steady-state levels of *Xist* transcripts (real-time RT–PCR; Figure 1D), which were increased approximately three- to five-fold as compared to the untargeted allele of the parental XX ES cell line (not shown; Morey *et al*, 2001). In the XLDp37 ES cell lines, a restored *Tsix*/*DXPas34* signal colocalized with a normal *Xist* pinpoint in 80% of the nuclei ($n = 200$), as visualized using RNA-FISH (XLDp37#5, Figure 1C, right panel; XLDp37#6, data not shown). In parallel, *Xist* RNA amounts were restored to normal in these cell lines (Figure 1D). These results probably reflect the repressive effect of *Tsix* on the steady-state levels of *Xist* RNA in undifferentiated ES cells, which has been previously reported (Luikenhuis *et al*, 2001; Morey *et al*, 2001; Sado *et al*, 2001; Stavropoulos *et al*, 2001).

We also wished to investigate whether the 37 kb DNA sequence, when re-inserted as naked DNA in our ES cell

line, is capable of reconstituting a native chromatin structure. To address this issue, we chose to analyse the distribution of histone H3 dimethylated on Lys-4, which marks transcriptionally active genomic regions (Turner, 2002), using ChIP and real-time quantitative PCR (Figure 1E). We focused our analysis on the *DXPas34* locus and the major initiation site for *Tsix*, because of the primary importance of this region in the regulation of XCI. No difference in the H3 Lys-4 methylation profile of this region in the XLDp37 ES cell lines was seen when compared to that of the wild-type XY CK35 ES cell line (XLDp37#5; Figure 1E; XLDp37#6, data not shown). This result validates our site-specific transgenesis approach by showing that the transgenic chromatin structure of the *DXPas34/Tsix* locus can be accurately reconstituted in complemented ES cells.

A 37 kb site-specific transgene rescues the counting process in Δ65 X0 ES cells

In order to investigate whether the 37 kb transgene was able to prevent the inappropriate initiation of XCI occurring in the differentiated XLD ES cells (Clerc and Avner, 1998), we analysed *Xist* expression in differentiated cells of both the deleted and complemented ES cell lines. A near-complete inhibition of the *Xist* upregulation was observed using real-time quantitative RT–PCR in embryoid bodies of the XLDp37 ES cell lines as compared to embryoid bodies of the parental

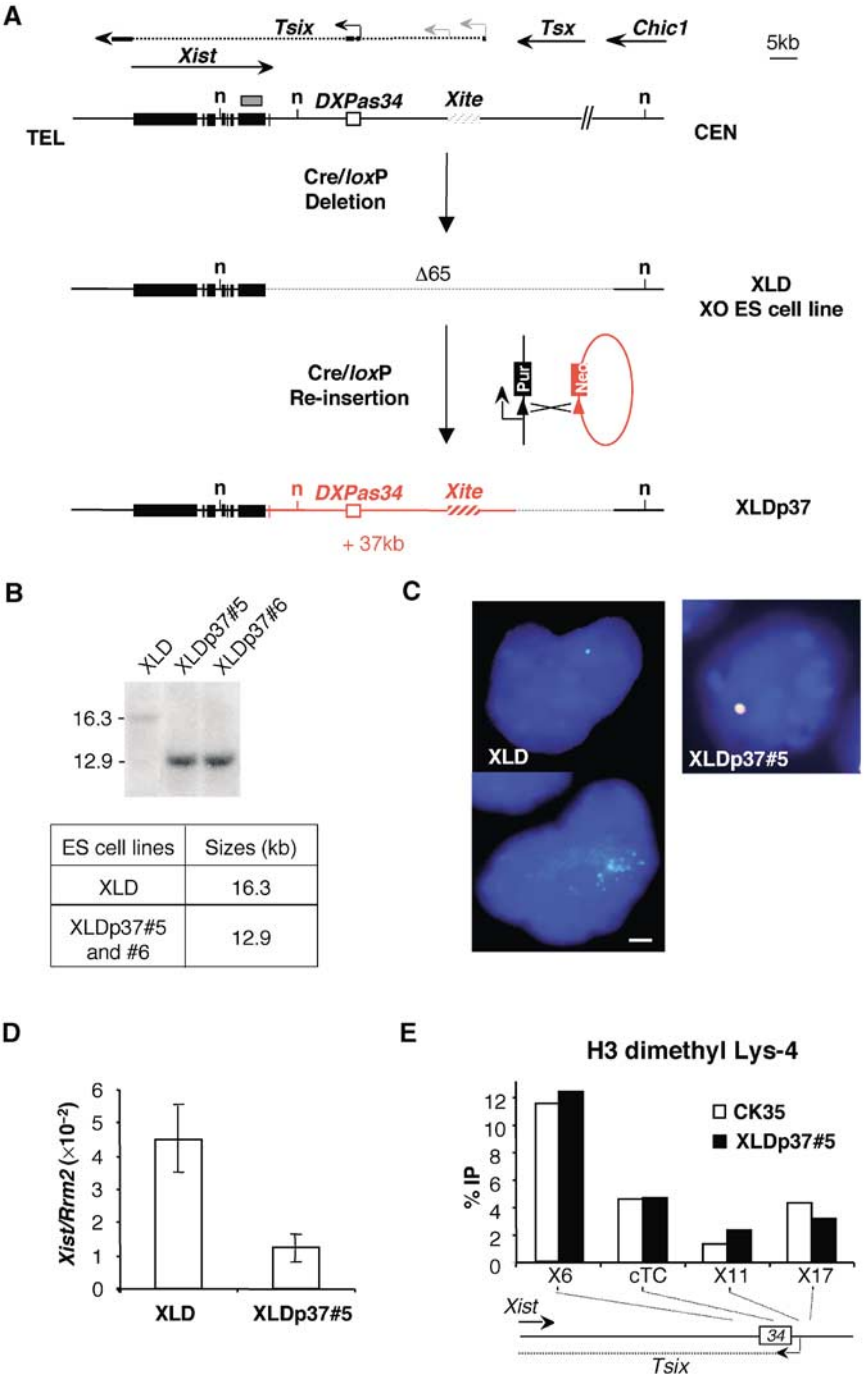

XLD ES cell line (XLDp37#5, Figure 2A; XLDp37#6, data not shown). To confirm this result using another differentiation method, we differentiated the cells using low-density cell culture conditions and performed quantitative RT–PCR and RNA-FISH analysis for *Xist* RNA in parallel at the same differentiation time point. After 3 days of differentiation under low cell density, the XLDp37 ES cell lines showed reduced steady-state levels of *Xist* RNA (XLDp37#5, Figure 2B; XLDp37#6, data not shown) as well as a dramatically decreased number of nuclei with a *Xist* domain (9% in XLDp37#5, $n=200$, Figure 2C; XLDp37#6, data not shown), as compared to the original XLD ES cell line (60%, $n=200$; Figure 2C).

Taken together, our results show that the inappropriate initiation of XCI occurring upon differentiation in the XLD ES cell line is prevented through site-specific reinsertion of a 37 kb DNA sequence encompassing *Tsix*, *DXPas34* and *Xite*. This indicates that elements involved in counting are located within this region. Abnormal counting has been suppressed in our XO ES cell line without prior passage through the germ line or the early stages of embryonic development. This suggests that counting is not irreversibly established in developmental stages preceding the ICM, and occurs in ES cells concurrently with or just prior to cell differentiation.

Construction of a 65 kb deletion 3′ to Xist in an XY ES cell line

It was of crucial importance to assess the role of the region 3′ to *Xist* in the counting pathway in ES cells since differences in X chromosome chromatin structure between XY and XX ES cells have been reported previously (O'Neill *et al*, 1999, 2003). We therefore decided to reproduce the original 65 kb deletion in the CK35 XY ES cells of 129/Sv origin through double targeting of *lox*P sites and cre expression (Figure 3A). Deleted clones were selected by the reconstitution of a functional puromycin gene flanked by *frt* sites, which was subsequently excised by expressing e*flp*, leaving a single 48 bp *frt* site (Schaft *et al*, 2001). The genomic structures of the deleted clones were confirmed in a Southern blot analysis (Figure 3B). In this study, two deleted clones with and two without the puromycin cassette were analysed and gave the same results. Data for a clone without the cassette are presented here.

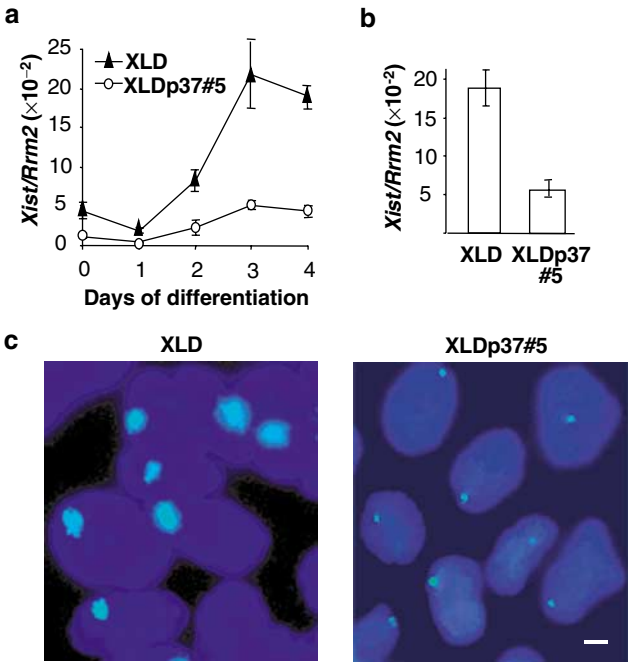

Figure 2 Inappropriate X-inactivation in the differentiated XLD XO ES cell line is prevented upon re-insertion of 37 kb of DNA lying 3′ to *Xist*. (**A**) Quantification of *Xist* RNAs (as described in Figure 1D) during differentiation into embryoid bodies. The steady-state level of *Xist* RNAs is upregulated during ES cell differentiation in XLD, but not in the XLDp37#5 ES cell line. (**B**) Quantification of *Xist* RNA standardized over *Rrm2* in the XLD and XLDp37#5 ES cells differentiated for 3 days in low-density cell culture. (**C**) In the same differentiation experiment as (B), *Xist* expression was assessed by RNA-FISH with the L510 probe (green) on DAPI-stained nuclei. The bar equals 25 μm. Respectively 60 and 9% of total nuclei exhibited a *Xist* domain ($n=200$) in XLD and XLDp37#5 ES cells differentiated for 3 days, consistent with a repression of *Xist* accumulation consecutive to the 37 kb complementation. Two independent differentiations of XLDp37#5 and of XLDp37#6 ES cell lines using the two differentiation systems gave similar results.

Figure 1 The 37 kb re-inserted DNA is refolded into a functional chromatin structure and restores normal *Xist* expression in undifferentiated XO ES cells. (**A**) Deletion and complementation strategies (Morey *et al*, 2001) in XO ES cells. The resulting 65-kb-deleted and 37-kb-complemented alleles are depicted underneath the map of the *Xist* locus. Arrows indicate the direction of transcription and arrowheads identify promoter sequences. Solid boxes, *Xist* exons; the plain and dotted lines show the exonic and intronic *Tsix* structure with major and minor *Tsix* promoters symbolized as black and grey arrowheads; hatched box, the *Xite* element; small arrow, intergenic antisense transcription constitutive of the *Xite* element (Ogawa and Lee, 2003); grey box, DNA probe; n, *Nde*I restriction sites relevant to the analysis in (B). (**B**) Southern-blot analysis and expected sizes of the *Nde*I restriction fragments detected with the DNA probe depicted in (A). Two re-inserted ES cell clones XLDp37#5 and XLDp37#6 were analysed. The structure of the XLDp37#5 and XLDp37#6 ES cell lines was also confirmed by PCRs at the boundaries of the 37 kb re-inserted region. (**C**) Two-colour RNA-FISH analysis for *Xist* (L510, green) and *DXPas34/Tsix* (Debrand *et al*, 1999) (red) on DAPI-stained undifferentiated XLD and XLDp37#5 ES cells. Overlapping green and red signals are seen as yellow. The bar equals 5 μm. The XLD ES cells show a faint *Xist* pinpoint (upper left panel) or scattered dots (in 15% of nuclei, $n=200$, down left panel), whereas a normal *Xist* pinpoint signal superimposed on a restored *DXPas34/Tsix* expression is detected in the undifferentiated XLDp37#5 ES cell line. (**D**) Dual real-time quantitative RT–PCR for *Xist* (spanning exons 5 and 6) and *Rrm2* (ribonucleoside diphosphate reductase M2) (Lee *et al*, 1999b) as a reporter in undifferentiated XLD and XLDp37#5 ES cell lines. Means ± SD ($n=4$) of *Xist* transcripts are standardized over *Rrm2* RNA and expressed in arbitrary units as previously described (Morey *et al*, 2001). Using the *18S* ribosomal RNA as an alternative reporter gave essentially similar results in all the experiments of this paper (data not shown). The elevated *Xist* level in XLD ES cells is restored to a normal low level in the XLDp37#5 ES cell line. This level is not significantly different from the amount of *Xist* transcripts originating from the same allele in the parental XX ES cell line. Similar results were obtained in at least two independent ES cell cultures for each ES cell line. (**E**) ChIP analysis of H3 Lys-4 dimethylation within the 37 kb re-inserted region in the undifferentiated XLDp37#5 ES cell line. Immunoprecipitated DNA was analysed by real-time quantitative PCR. The location of the primer pairs is represented on the small map below the graph. A 5 kb region around the *DXPas34* locus, which has a crucial function in the regulation of the *Xist* locus, was analysed. The graphs show the %IP obtained for each primer pairs and each ES cell line. CK35 and XLDp37 harbour very similar H3 Lys-4 dimethylation profiles indicative of an accurate chromatin refolding of the 37 kb region in the XLDp37#5 ES cell line. All experiments described in this figure have been carried out in parallel on the XLDp37#6 ES cell line with essentially identical results (data not shown).

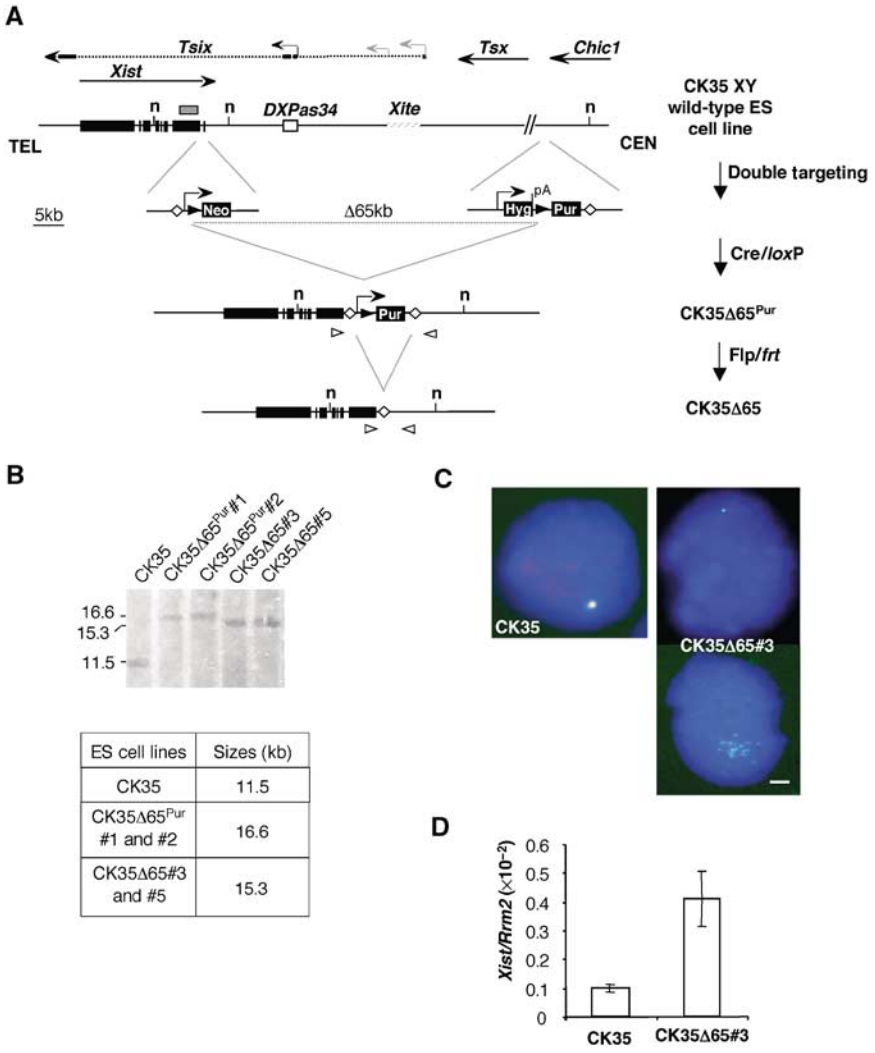

ES cell lines	Sizes (kb)
CK35	11.5
CK35Δ65^{Pur} #1 and #2	16.6
CK35Δ65#3 and #5	15.3

Figure 3 Deleting 65 kb 3′ of *Xist* in ES cells results in *Xist* RNA upregulation and alters *Xist* RNA distribution within the nuclei of undifferentiated ES cells. (**A**) Strategy for the 65 kb deletion in CK35 XY ES cells. Targeting vectors and the structures resulting after Cre and Flp expression are shown. Black triangles, *lox*P sites; open diamonds, *frt* sites. Open triangles indicate the primer pair (DC651Up-Del1Lo) used for the PCR screening of the deleted clones. Arrowheads represent promoter sequences and pA, a polyadenylation signal. (**B**) Southern-blot analysis of the CK35Δ65 ES cells. The analysis was performed using the *Nde*I restriction enzyme (n, *Nde*I restriction sites) and a probe located in *Xist* exon 7 (grey box). The flp/*frt* cassette excision was carried out on two independent cre/*lox*P-deleted clones CK35Δ65^{Pur}#1 and CK35Δ65^{Pur}#2, and gave rise, respectively, to cell lines CK35Δ65#3 and CK35Δ65#5. The Southern-blot analysis confirmed the genomic structure of the deleted alleles. (**C**) RNA-FISH for *Xist* (green) and *DXPas34/Tsix* (red) on CK35 and CK35Δ65#3 on DAPI-stained nuclei of undifferentiated ES cells. The bar equals 5 μm. CK35Δ65#3 ES cells exhibit a reduced *Xist* pinpoint (upper right panel) or faint *Xist* RNA signals diffused around the *Xist* transcription site (down right panel). (**D**) Quantification of *Xist* transcripts in undifferentiated CK35 and CK35Δ65#3 ES cell lines using quantitative real-time RT–PCR for *Xist* and the *Rrm2* reporter gene. CK35Δ65#3 ES cells show a four-fold increase in *Xist* steady-state levels compared to the wild-type CK35 ES cell line. Similar results were obtained for the CK35Δ65#5 ES cell line.

Using RNA-FISH, *Xist* was detected as a faint pinpoint or as a collection of weak scattered signals in the CK35Δ65 undifferentiated ES cell lines (CK35Δ65#3, Figure 3C right panels; CK35Δ65#5, data not shown). *Xist* RNA steady-state levels were four-fold higher in the deleted CK35Δ65 ES cells compared to the wild-type CK35 ES cell line (Figure 3D), consistent with the de-repression of *Xist* consecutive to the lack of antisense transcription in CK35Δ65 ES cells. We note incidentally the low levels of *Xist* RNA in the CK35 XY ES cell line as compared to other wild-type ES cell lines, which likely results from differences in genetic backgrounds (data not shown). We conclude that undifferentiated ES cells deleted for 65 kb downstream to *Xist* show a phenotype essentially identical to the XLD ES cell line bearing the same deletion in an XO female context.

A 65 kb deletion located 3′ to Xist results in XCI in XY differentiated ES cells

In order to analyse the impact of the 65 kb deletion in ES cells on the counting process, CK35Δ65 ES cells were differentiated into embryoid bodies and analysed for *Xist* RNA expression. Using quantitative RT–PCR, a greater than 40-fold upregulation of *Xist* expression after 3 days of differentiation was observed (CK35Δ65#3, Figure 4A; CK35Δ65#5, data not shown). This corresponds to a 20-fold difference in the levels of *Xist* RNA between CK35Δ65#3 and parental CK35 differentiated cells at day 3 (Figure 4A). A highly significant increase in the steady-state level of *Xist* RNA in the CK35Δ65#3 cell line as compared to the CK35 ES cell line was also observed at day 3 of differentiation under low-density cell culture conditions (Figure 4B). We then

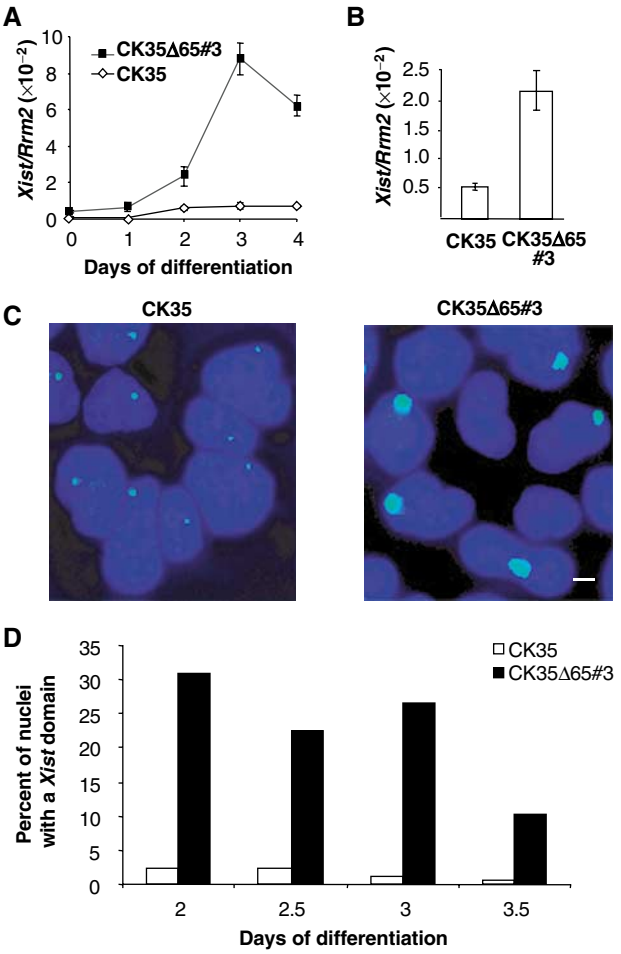

Figure 4 Inappropriate initiation of X-inactivation occurs in differentiated CK35Δ65 ES cells. (**A**) *Xist* expression measured in real-time quantitative RT–PCR during ES cell differentiation into embryoid bodies. CK35Δ65#3 ES cell line shows an increase in *Xist* RNA levels during differentiation into embryoid bodies. (**B**) *Xist* steady state levels measured by real-time RT–PCR and normalized using the *Rrm2* reporter gene in CK35 and CK35Δ65#3 ES cells differentiated for 3 days in low-density cell culture. (**C**) In the same differentiation experiment, *Xist* RNA-FISH on DAPI-stained nuclei of CK35 and CK35Δ65#3 ES cell lines differentiated for 3 days. The bar equals 25 μm. High levels of *Xist* expression are associated with inappropriate *Xist* accumulation at the $X^{\Delta 65}$ in the CK35Δ65#3 ES cell line. (**D**) Kinetics of *Xist* accumulation during ES cell differentiation under low-density cell culture conditions. The proportion of nuclei showing an accumulation of *Xist* RNA between days 2 and 3.5 of differentiation is illustrated. A total of 100–200 nuclei were scored for each differentiation time point. Two independent experiments for CK35Δ65#3 and CK35Δ65#5 and CK35Δ65^{Pur}#1 and CK35Δ65^{Pur}#2 using both differentiation systems gave similar results.

determined the kinetics of appearance of *Xist* accumulations using RNA-FISH. Essentially no *Xist* accumulations could be detected in wild-type CK35 differentiated ES cells (Figure 4C and D). In contrast, in the CK35Δ65#3 ES cell line, 30% of the cells exhibited a mature *Xist* domain as early as day 2 of differentiation (CK35Δ65#3, Figure 4D; CK35Δ65#5, data not shown). Bearing in mind that the lack of synchronization of the cell differentiation process usually results in less than 50% of cells with a *Xist* domain at day 2 (see, e.g., Morey *et al*, 2001; Plath *et al*, 2003), this suggests that ES cells carrying the 65 kb deletion, differentiated for short times, have a capacity to initiate XCI comparable to that of wild-type XX ES cells.

In order to test whether *Xist* accumulations on the $X^{\Delta 65}$ were associated with transcriptional silencing, we performed RNA-FISH with probes for the X-linked genes *Chic1* and *Mecp2* located 12.4 cM distal to the *Xic*, in CK35Δ65 differentiated ES cell lines. A large and significant percentage of *Xist* domains lacked an associated *Chic1* (Figure 5A–C) or *Mecp2* (Figure 5D–F) signal. These data indicate that *Xist* RNA upregulation from the $X^{\Delta 65}$ in differentiated ES cells results in the long-range silencing of X-linked genes. Silencing of the single $X^{\Delta 65}$ chromosome is likely to be responsible for the cell mortality, which is most probably the cause of the decrease in the number of *Xist* domains observed at later differentiation time points (post 3 days) with the CK35Δ65 ES cell lines (CK35Δ65#3, Figure 4D; CK35Δ65#5, data not shown).

Our data establish that the 65 kb deletion results in efficient initiation of XCI both in an XO ES cell line of 129/C3 H.Pgk1a background (the targeted *Xic* being of Pgk1a origin) and in a 129 XY ES cell line. This underlies the specificity of the 65 kb deletion phenotype, which is independent of both the genetic background and the XY/XX nature of the cell lines.

H3 Lys-9 methylation hotspot lying 5′ to Xist is unaffected by the 65 kb deletion 3′ to Xist in ES cells

In an attempt to characterize the function of the region 3′ to *Xist* and its interaction(s) with other parts of the *Xic*, we investigated whether the H3 Lys-9 methylation hotspot extending upstream of the *Xist* gene (Heard *et al*, 2001) would be affected by the 65 kb deletion 3′ to *Xist*. ChIP experiments were performed in parallel on the CK35 and CK35Δ65 ES cell lines, and explored a region encompassing 150 kb upstream of the *Xist* gene. Wild-type CK35 ES cells displayed high levels of H3 Lys-9 dimethylation over the hotspot region, similarly to what was previously described (Heard *et al*, 2001) (Figure 6A). Such high levels of H3 Lys-9 dimethylation were also observed 5′ to *Xist* in the deleted ES cell lines (Figure 6A). The slight differences seen at some positions in Figure 6A could not be reproduced in other ChIP experiments (data not shown). We conclude that the levels of H3 Lys-9 dimethylation in the hotspot region are unaffected by the 65 kb deletion and therefore are not controlled by *Tsix*, by *Xite*, or the element involved in counting that we have identified.

The region 3′ to Xist controls H3 Lys-4 dimethylation within the Xist gene without affecting H3 Lys-9 methylation in ES cells

To further characterize the role of the region lying 3′ to *Xist*, we examined the levels of H3 Lys-4 and Lys-9 dimethylation within the *Xist* gene in the CK35, CK35Δ65, XLD and XLDp37 ES cell lines.

The analysis of H3 Lys-4 dimethylation at the *Xist* locus gave striking results. In wild-type CK35 ES cells, the body of the *Xist* gene (positions Xe1b, Xg and Xe7, located respectively within *Xist* exon 1, exon 5–intron 5 junction and exon 7, Figure 6B) was associated with high levels of H3 dimethyl Lys-4 as compared to a position 7 kb upstream of the *Xist* promoter (position X3; Figure 6B). The 65 kb deletion 3′ to *Xist* affected dramatically H3 Lys-4 dimethylation levels within the *Xist* gene, as a near-complete loss of methylation was

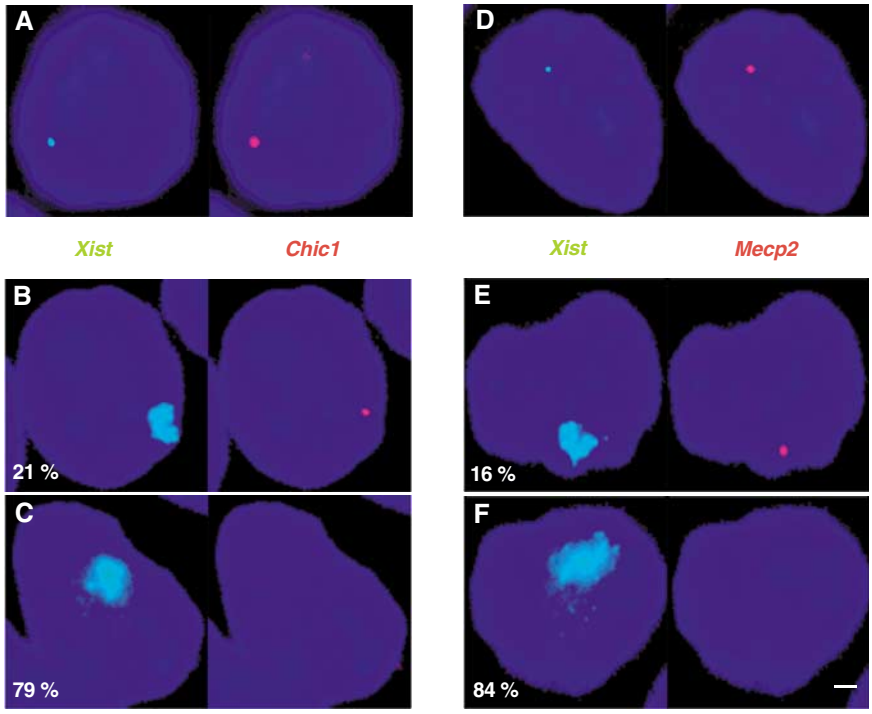

Figure 5 Inappropriate *Xist* accumulations in CK35Δ65 differentiated ES cells result in efficient X-linked genes silencing. (**A–C**) Silencing of the *Chic1* gene. Two-colour RNA-FISH using probes for *Chic1* (red) and *Xist* (green) in the CK35Δ65#3 ES cell line differentiated for 3 days in low-density cell culture. (A) shows an example of a nucleus where XCI has not yet occurred. In all, 93% of the cells presented a detectable *Chic1* signal. To evaluate silencing, the number of nuclei ($n = 200$) displaying a high-level *Xist* expression associated (B) or not (C) with a *Chic1* signal was determined. Percentages are indicated. The bar equals 5 μm. (**D–F**) Silencing of the *Mecp2* gene. A probe specific for the *Mecp2* gene (red) was used to perform an analysis identical to that in (A–C). A 75% frequency of detection of *Mecp2* was obtained in cells in which initiation of XCI had not yet occurred (D), whereas only 16% of the cells with an *Xist* RNA–FISH domain demonstrated a signal for *Mecp2* (**E**).

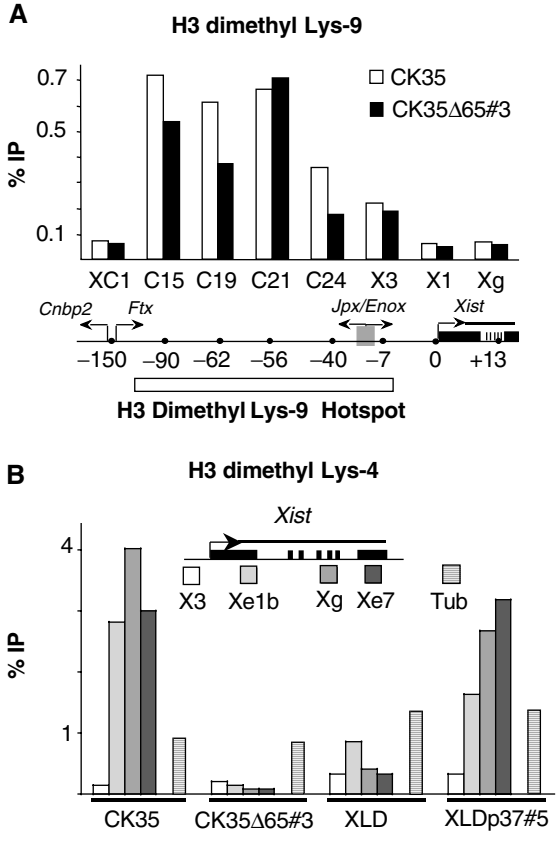

detected in the CK35Δ65#3 cell line (positions Xe1, Xg and Xe7; Figure 6B). Low levels of H3 Lys-4 dimethylation were also observed in the *Xist* gene in the 65-kb-deleted XLD ES

Figure 6 Effects of mutations 3′ to *Xist* on H3 Lys-9 and Lys-4 dimethylation 5′ and within the *Xist* gene in ES cells. (**A**) ChIP analysis of H3 Lys-9 dimethylation in the hotspot region and in the *Xist* locus in the CK35 and CK35Δ65 ES cell lines. The immunoprecipitated chromatin was analysed by real-time quantitative PCR using assays spanning over 150 kb of the H3 Lys-9 dimethyl hotspot region 5′ to *Xist* (Heard *et al*, 2001). Two primer pairs located within the *Xist* gene were also used (X1 and Xg). Coordinates of the assays relative to the *Xist* P1 promoter are indicated in kilobases. High levels of H3 lys-9 methylation over a 150 kb region 5′ to *Xist* were observed in both the CK35 and the CK35Δ65#3 ES cell lines. No significant differences between the CK35 and CK35Δ65#3 ES cell lines in the levels of H3 Lys-9 methylation at the positions tested could be reproducibly observed in the course of repeat experiments. Results from a single representative experiment are shown. (**B**) ChIP analysis of H3 Lys-4 dimethylation within the *Xist* gene in wild-type and mutated ES cells. PCR assay X3 is located 7 kb upstream of the *Xist* promoter P1. PCR assays Xe1b, Xg and Xe7 are located, respectively, within *Xist* exon 1, exon 5–intron 5 junction and exon 7. The ChIP efficiencies are controlled using PCR assays located within the *α-tubulin* (stripped columns), *myc* and *G6pd* genes (not shown). In the CK35 wild-type ES cell line, high levels of H3 Lys-4 methylation were observed within the *Xist* gene (assays Xe1b, Xg and Xe7), but not upstream of it (assay X3). A drastic loss of H3 Lys-4 dimethylation is observed in the *Xist* gene of the 65-kb-deleted X in the CK35Δ65#3 ES cell line. The levels of H3 Lys-4 dimethylation are similarly low in the *Xist* gene in the XLD ES cell line, and increased in the complemented XLDp37#5 ES cell line. Three independent experiments provided results essentially identical to the example shown here.

cell line and, interestingly, the H3 Lys-4 dimethylation levels were significantly increased by the 37 kb add back present in XLDp37 ES cells (Figure 6B). Our results clearly establish that the 37 kb region downstream to *Xist* controls the H3 Lys-4 dimethylation in the *Xist* gene. This effect seems to be restricted to within the *Xist* gene itself, as no difference could be observed at a position 7 kb 5′ to *Xist*. In addition, we found comparable low levels of H3 Lys-9 methylation at the *Xist* locus (positions X1 and Xg; Figure 6A) in the CK35 wild-type and CK35Δ65 ES cell lines, suggesting that the region 3′ to *Xist* has no impact on H3 Lys-9 methylation within the *Xist* gene.

Altogether, our results establish that the region downstream to *Xist* specifically controls the levels of H3 Lys-4 dimethylation within the *Xist* gene without affecting the levels of H3 Lys-9 methylation.

Discussion

Our study explores the temporal and mechanistical aspects of the counting process. We report on the phenotypic rescue of counting through site-specific transgenesis in an XO ES cell line deleted for a 65 kb region downstream to *Xist* and defective for normal counting. The fact that normal counting could be rescued has important implications for the timing of the counting process during development and restricts the location for the elements of counting to 20 kb of genomic DNA. In parallel, we have generated a 65 kb deletion 3′ to *Xist* in an XY ES cell line and described its capacity to efficiently undergo inappropriate silencing upon differentiation. Importantly, we show that the 37 kb region closest to the 3′ end of the *Xist* gene specifically controls H3 Lys-4 dimethylation within the *Xist* gene, but not H3 Lys-9 methylation either at the H3 Lys-9 hotspot lying 5′ to *Xist* or within the *Xist* gene itself.

Three mutations targeting *Tsix* (Lee *et al*, 1999b; Luikenhuis *et al*, 2001; Sado *et al*, 2001) have previously demonstrated only minor or no effects on the initiation of XCI in differentiated male ES cells. These results differ strikingly from our observation of efficient XCI in an XO ES cell line bearing a 65 kb deletion encompassing *Tsix*, which was derived from an XX ES cell line (this work and Clerc and Avner (1998)). This has led Lee *et al* (1999b) to suggest that a 'competence factor' strictly required for the initiation of XCI might be produced in XX cells. According to this hypothesis, XO ES cells would possess this factor and be competent to initiate XCI due to their XX origin. In contrast, XY ES cells would lack this factor and should therefore be unable to undergo XCI even in the presence of the mutation. Our observation that the 65 kb deletion induces XCI with high efficiency in XY differentiating ES cells excludes the involvement of such a 'competence factor' in the differential programming of XCI in males and females. The similar phenotype of the 65 kb deletion in XO and XY differentiated ES cells also suggests that the differential chromatin marks present on the X chromosomes in male and female ES cells (O'Neill *et al*, 1999, 2003) can have, if any, only a minor influence on XY/XX XCI differential programming. Taken together, our results indicate that the phenotypic differences between the various mutations can likely be attributed solely to the nature of the mutations and not to parameters specific to the ES cell lines like the sex of the embryo of origin or its genetic background. Our data strongly support a role for the region 3′ to *Xist* in the counting pathway.

The re-establishment of normal counting obtained on reinsertion of cloned DNA into ES cells implies that ES cells possess all the factors necessary for functional reconstitution. Our data demonstrate clearly that X chromosomes cannot have been definitively precounted at embryonic stages preceding that of the ICM from which ES cells are derived, and that at least part of the counting process operates at the time of cell differentiation. This finding is of major importance for subsequent experimentation aimed at identifying precisely the 'counting element' that will exploit the ES cell system. Furthermore, our site-specific transgenesis approach locates the elements of counting to within the 37 kb region 3′ to *Xist*. Both *Tsix* and *Xite*, which lie within this interval, have been shown respectively by a 3.7 kb and by a 12.5 kb deletion not to be directly involved in the counting mechanism (Lee *et al*, 1999a; Ogawa and Lee, 2003). We, therefore, propose that the element important for counting lies within a 20 kb bipartite region depicted in Figure 7. Interestingly, comparative sequence analysis has identified a 2 kb region of mouse/human conservation (80610–82632 of Genbank no. X99946), located proximal to *DXPas34* (Chureau *et al*, 2002), which, based on our results, must constitute an interesting candidate for a function in the counting pathway. The precise nature of this function has yet to be determined. Counting seems to involve both a sensing of the X chromosome number relative to cell ploidy and the output of this information into the control of the initiation of XCI. As the degree of integration of these two steps is still unclear, the element located in the region that we have identified might be the 'counting element' that is postulated to interact with a 'blocking factor', or an effector acting downstream, which would repress *in cis* the initiation of XCI. It is intriguing that *Tsix*, a well-characterized

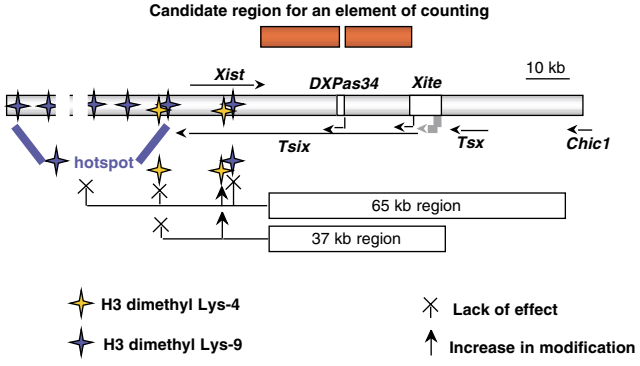

Figure 7 Schematic representation of the roles of the region 3′ to *Xist* in counting and in control of H3 Lys-9 and Lys-4 dimethylation at the *Xist* locus. The schema depicts the *Xist* locus, as well as the *DXPas34/Tsix* and *Xite* elements, which have been previously excluded from having a function in counting. The location of the bipartite 20 kb region identified in this study as containing an element of counting is shown above the central schema. The positions tested for histone H3 Lys-9 and Lys-4 dimethylation are, respectively, indicated by blue and yellow stars. The role of the region lying 3′ to *Xist* in histone H3 modification is illustrated in the lower part of the diagram. In ES cells, the 65 kb region has no effect on H3 Lys-9 dimethylation in either the hotspot region or the *Xist* locus. In contrast, the region 3′ to *Xist* targets the deposition of the Lys-4 dimethyl form of H3 to within the body of the *Xist* gene. This regulation is specifically supported by the proximal 37 kb subregion of the 65 kb span.

repressor *in cis* of the initiation of XCI (Luikenhuis *et al*, 2001; Morey *et al*, 2001; Stavropoulos *et al*, 2001), has been excluded for a function in counting (Lee *et al*, 1999b). We must therefore postulate the existence of yet another repressor element or of the 'counting element' itself within the 20 kb region that we have identified.

Our observation of a differential effect of the region 3′ to *Xist* on H3 Lys-4 and Lys-9 methylation within the *Xist* gene itself emphasizes the complexity of the regulatory process involving the *Xist* locus, which is summarized in Figure 7. We observed no significant effect of the region 3′ to *Xist* on H3 Lys-9 methylation either within *Xist* or within a region extending 5′ to *Xist*, which is part of an H3 Lys-9 methylation hotspot proposed to act as a nucleation centre for the spreading of XCI. This indicates that the H3 Lys-9 methylation hotspot is not acting downstream of the element of counting present in the region 3′ to *Xist* and is likely independent of *Xist* RNA steady-state levels, which are elevated in the CK35Δ65 ES cell lines. Conversely, the 65 kb deletion induced a dramatic loss of H3 Lys-4 dimethylation restricted to the *Xist* gene itself. H3 Lys-4 and Lys-9 methylations have frequently been described as mirrors of each other (Turner, 2002), and a dissociation of this inverse correlation has been reported only rarely (Yan *et al*, 2003). Such a lack of correlation between H3 Lys-4 and Lys-9 dimethylations may therefore be specific to particular loci, including the *Xist* gene.

As shown by our site-specific transgenesis approach, the control of H3 Lys-4 methylation is primarily exerted by the 37 kb domain, which is responsible both for antisense transcription within *Xist* and for normal counting. It remains for the moment an open and important question as to whether H3 Lys-4 methylation within the *Xist* gene is linked to antisense transcription, or counting, or both. In an attempt to explore this question, we have looked at the *Xist* H3 Lys-4 methylation profile in our previously described D102 and c16 XX ES cell lines (Clerc and Avner, 1998; Morey *et al*, 2001). These cell lines both carry a wild-type X chromosome accompanied, respectively, by a 65-kb-deleted X or a 65-kb-deleted X chromosome complemented for the proximal 16 kb consisting in the *Tsix* antisense transcription unit. Our preliminary results suggest that the H3 Lys-4 methylation within the *Xist* gene, lost on deletion of the 65 kb, is partially recovered after the *Tsix* restoration (data not shown). Although further experimental validations would be necessary, this leads us to favour the hypothesis of an association between antisense transcription and the chromatin remodelling we have detected. Indeed, transcriptionally active chromatin domains generally show elevated levels of H3 Lys-4 dimethylation and, in yeast, this mark results at least in part from the association of the Set1 H3 methyl transferase with the elongating RNA polII (Krogan *et al*, 2003; Ng *et al*, 2003). Our results show that H3 Lys-4 dimethylation is lost in the 65-kb-deleted allele, despite ongoing *Xist* sense transcription. This suggests that the *Tsix*, but not the *Xist*, transcriptional machinery might recruit an H3 lys-4 methyl transferase. A more speculative possibility is that an H3 Lys-4 methyl transferase could be recruited to the *Xist* gene as a result of the sense/antisense transcriptional activity within the locus, using a putative nuclear RNAi pathway reminiscent of the one existing in *Schizosaccharomyces pombe* (Volpe *et al*, 2002). Finally, the link between H3 Lys-4 dimethylation within *Xist* and the counting process leads us to postulate, for the first time, a role of genomic elements within the *Xist* gene itself in counting. Our results indicate that Lys-4 methylation within *Xist* is associated with an inhibition of the initiation of XCI and a functional counting process. It is conceivable that Lys-4 dimethylation within the *Xist* gene, by creating an open chromatin conformation, could potentiate the interaction of this domain with regulatory factors involved in preventing the initiation of XCI, and thereby mediate counting. Indeed, a function ensured by H3 Lys-4 dimethylation may well be to regulate the accessibility of *cis*-acting DNA elements, as suggested by recent findings in the immunoglobulin heavy-chain locus (Morshead *et al*, 2003). Further work will be required to explore these exciting avenues and for a complete understanding of the counting process of X chromosome inactivation.

Materials and methods

ES cell site-specific re-insertion

The XLD ES cell line was electroporated using a mixture of the cre-expressing plasmid pOG231 (Clerc and Avner, 1998) and the pGln37 plasmid (see below). The complemented clones were selected for the reconstitution of a functional neomycin cassette, and neomycin-resistant colonies were PCR screened as previously described (Morey *et al*, 2001). After preliminary FISH analysis for X aneuploidy, two positive clones were extended and characterized. The pGln37 plasmid was obtained by inserting the *lox*P-neomycin ORF from the pC3Nleo (Clerc and Avner, 1998) plasmid and the 37 kb *Cla*I fragment from a BAC clone encompassing *DXPas34* (Chureau *et al*, 2002) into a plasmid bearing the low-copy replication origin of the pLG339 vector (Stoker *et al*, 1982) and the ampicillin resistance gene.

Targeted deletions

The genomic targeting for the 65 kb deletion was realized on the CK35 male ES cell line originating from the 129 mouse strain. ES cell transfections and selections of recombinants were performed as previously described for the HP3.10 ES cell line (Clerc and Avner, 1998). Both proximal and distal homology regions were generated as previously described (Clerc and Avner, 1998). The CK35Δ65^{Pur} ES cell clones were selected for the reconstitution of the puromycin gene (1 μg/ml) and were PCR screened (primer pair D651Up-Del1Lo; see Figure 3A). The puromycin excision was carried out by lipofecting two independent CK35Δ65^{Pur} ES cell clones with the pCAGGS-FLPe supercoiled flp-expressing plasmid (Schaft *et al*, 2001). Two CK35Δ65 ES cell clones derived from each of the two CK35Δ65^{Pur} clones were selected on the basis of their sensitivity to puromycin and using the PCR screening assay, which gives a smaller product after the loss of the puromycin gene.

RNA-FISH

The preparation of nuclei, hybridization and washes were performed as described (Clerc and Avner, 1998) using DNA probes labelled by nick translation with Spectrum Red or Green dUTP (Vysis, Downer Grove, IL, USA). A Zeiss Axioplan fluorescence microscope with a Quantix CCD camera (Photometrix) and the SmartCapture 2 software (Digital Scientific) were used for image acquisition. All the probes used in this study have been previously described (Clerc and Avner, 1998; Debrand *et al*, 1999; Heard *et al*, 1999).

Real-time quantitative RT–PCR

Quantitative real-time PCR measurements of *Xist* random primed cDNA were performed using TaqMan fluorescent probes and TaqMan Universal PCR mix (Perkin-Elmer Applied Biosystem) on ABI Prism 7700 (Perkin-Elmer Applied Biosystem). *Xist* cDNA quantitations were internally standardized against the endogenous *18S* cDNA or against the *Rrm2* cDNA. The PCR assays for *Xist* and *18S* genes were the same as previously described (Morey *et al*, 2001). For *Rrm2*, a new system was set (primer pair Rrm1F-Rrm1R, TaqMan probe Rrm2), which spans an exonic junction to prevent any contaminating amplification of genomic DNA. The lack of

interference between the amplification and detection systems for *Xist* and *Rrm2* was verified. The specificity of each PCR was checked by running in parallel a PCR on an RT reaction lacking the enzyme.

ES cell culture and in vitro differentiation

ES cells were grown in DMEM (GIBCO), 15% foetal calf serum (FCS; ES cell grade, GIBCO) and 1000 U/ml leukemia inhibitory factor (LIF; Chemicon) on male embryonic feeders for two passages prior to analysis. For the ChIP analysis, ES cells were cultured on gelatin-coated flasks in the absence of feeder cells (Heard *et al*, 2001). ES cell differentiation into embryoid bodies was performed as previously described (Morey *et al*, 2001). For ES cell differentiation under low-density cell culture conditions, ES cells were plated at 7000 cells/cm^2 on gelatin-coated plates for RNA extraction or on gelatinized slide flasks (Nunc) for RNA-FISH analysis without feeders, and grown for 4 days in a medium with 10% of FCS without LIF. The medium was changed daily throughout differentiation. All ES cell lines exhibited morphological features of differentiated cells after 2 days of culture under these conditions and only low levels of cell mortality before 4 days of differentiation.

Chromatin immunoprecipitation (ChIP)

Immunoprecipitations were performed using a dimethylated H3 Lys-4 antibody or a dimethylated H3 Lys-9 antibody (Upstate Biotechnology, Lake Placid, NY, USA), as described previously (Heard *et al*, 2001). Cells were crosslinked with 1% formaldehyde for 15 min at RT. Isolated nuclei were sonicated to an average length of 300–1000 bp. Immunoprecipitated DNA and input DNA were analysed by real-time PCR using SYBR Green Universal Mix and an ABI Prism 7700 (Perkin-Elmer Applied Biosystem). Each PCR was run in triplicate. For standardization, the results are represented as a percentage of immunoprecipitation, calculated by dividing the average value of the IP by the average value of the corresponding input, both values being first normalized by the dilution factor. Each experiment was repeated on independent chromatin extracts a total of three times.

Supplementary data

Supplementary data are available at *The EMBO Journal* Online.

Acknowledgements

CM is a doctoral fellow supported by the French Ministry for Scientific Research and by the Association pour la Recherche contre le Cancer (ARC). This work was supported by grants to PA from the ARC.

References

Chureau C, Prissette M, Bourdet A, Barbe V, Cattolico L, Jones L, Eggen A, Avner P, Duret L (2002) Comparative sequence analysis of the X-inactivation center region in mouse, human, and bovine. *Genome Res* **12:** 894–908

Clerc P, Avner P (1998) Role of the region 3′ to Xist exon 6 in the counting process of X-chromosome inactivation. *Nat Genet* **19:** 249–253

Debrand E, Chureau C, Arnaud D, Avner P, Heard E (1999) Functional analysis of the *DXPas34* locus, a 3′ regulator of Xist expression. *Mol Cell Biol* **19:** 8513–8525

Gartler SM, Riggs AD (1983) Mammalian X-chromosome inactivation. *Annu Rev Genet* **17:** 155–190

Heard E, Mongelard F, Arnaud D, Avner P (1999) *Xist* yeast artificial chromosome transgenes function as X-inactivation centers only in multicopy arrays and not as single copies. *Mol Cell Biol* **19:** 3156–3166

Heard E, Rougeulle C, Arnaud D, Avner P, Allis CD, Spector DL (2001) Methylation of histone H3 at Lys-9 is an early mark on the X chromosome during X inactivation. *Cell* **107:** 727–738

Krogan NJ, Dover J, Wood A, Schneider J, Heidt J, Boateng MA, Dean K, Ryan OW, Golshani A, Johnston M, Greenblatt JF, Shilatifard A (2003) The Paf1 complex is required for histone H3 methylation by COMPASS and Dot1p: linking transcriptional elongation to histone methylation. *Mol Cell* **11:** 721–729

Lee JT, Davidow LS, Warshawsky D (1999a) Tsix, a gene antisense to Xist at the X-inactivation centre. *Nat Genet* **21:** 400–404

Lee JT, Lu N, Keohane AM, O'Neill LP, Belyaev ND, Lavender JS, Turner BM (1999b) Targeted mutagenesis of Tsix leads to non-random X inactivation. *Cell* **99:** 47–57

Luikenhuis S, Wutz A, Jaenisch R (2001) Antisense transcription through the *Xis*t locus mediates *Tsix* function in embryonic stem cells. *Mol Cell Biol* **21:** 8512–8520

Mermoud JE, Popova B, Peters AHFM, Jenuwein T, Brockdorff N (2002) Histone H3 lysine 9 methylation occurs rapidly at the onset of random X chromosome inactivation. *Curr Biol* **12:** 247–251

Morey C, Arnaud D, Avner P, Clerc P (2001) Tsix-mediated repression of *Xist* accumulation is not sufficient for normal random X inactivation. *Hum Mol Genet* **10:** 1403–1411

Morshead KB, Ciccone DN, Taverna SD, Allis CD, Oettinger MA (2003) Antigen receptor loci poised for V(D)J rearrangement are broadly associated with BRG1 and flanked by peaks of histone H3 dimethylated at lysine 4. *Proc Natl Acad Sci USA* **100:** 11577–11582

Ng HH, Robert F, Young RA, Struhl K (2003) Targeted recruitment of Set1 histone methylase by elongating Pol II provides a localized mark and memory of recent transcriptional activity. *Mol Cell* **11:** 709–719

O'Neill LP, Keohane AM, Lavender JS, McCabe V, Heard E, Avner P, Brockdorff N, Turner BM (1999) A developmental switch in H4 acetylation upstream of Xist plays a role in X chromosome inactivation. *EMBO J* **18:** 2897–2907

O'Neill LP, Randall TE, Lavender J, Spotswood HT, Lee JT, Turner BM (2003) X-linked genes in female embryonic stem cells carry an epigenetic mark prior to the onset of X inactivation. *Hum Mol Genet* **12:** 1783–1790

Ogawa Y, Lee JT (2003) Xite, X-inactivation intergenic transcription elements that regulate the probability of choice. *Mol Cell* **11:** 731–743

Panning B, Dausman J, Jaenisch R, Avner P, Brockdorff N, Turner BM (1997) X chromosome inactivation is mediated by Xist RNA stabilization. *Cell* **90:** 907–916

Panning B, Jaenisch R (1996) DNA hypomethylation can activate *Xist* expression and silence X-linked genes. *Genes Dev* **10:** 1991–2002

Penny GD, Kay GF, Sheardown SA, Rastan S, Brockdorff N (1996) Requirement for *Xist* in X chromosome inactivation. *Nature* **379:** 131–137

Plath K, Fang J, Mlynarczyk-Evans SK, Cao R, Worringer KA, Wang H, de la Cruz CC, Otte AP, Panning B, Zhang Y (2003) Role of histone H3 lysine 27 methylation in X inactivation. *Science* **300:** 131–135

Rastan S, Robertson EJ, Rasmussen TP, Mastrangelo MA, Eden A, Pehrson JR, Jaenisch R (1985) X-chromosome deletions in embryo-derived (EK) cell lines associated with lack of X-chromosome inactivation. *J Embryol Exp Morphol* **90:** 379–388

Rice JC, Allis CD (2001) Code of silence. *Nature* **414:** 258–261

Sado T, Li E, Sasaki H (2002) Effect of *TSIX* disruption on *XIST* expression in male ES cells. *Cytogenet Genome Res* **99:** 115–118

Sado T, Wang Z, Sasaki H, Li E (2001) Regulation of imprinted X-chromosome inactivation in mice by Tsix. *Development (Cambridge, England)* **128:** 1275–1286

Schaft J, Ashery-Padan R, van der Hoeven F, Gruss P, Stewart AF (2001) Efficient FLP recombination in mouse ES cells and oocytes. *Genesis* **31:** 6–10

Sheardown SA, Duthie SM, Johnston CM, Newall AE, Formstone EJ, Arkell RM, Nesterova TB, Alghisi GC, Rastan S, Brockdorff N (1997) Stabilization of Xist RNA mediates initiation of X chromosome inactivation. *Cell* **91:** 99–107

Silva J, Mak W, Zvetkova I, Appanah R, Nesterova TB, Webster Z, Peters AH, Jenuwein T, Otte AP, Brockdorff N (2003) Establishment of histone h3 methylation on the inactive x

chromosome requires transient recruitment of eed-enx1 polycomb group complexes. *Dev Cell* **4:** 481–495

Stavropoulos N, Lu N, Lee JT (2001) A functional role for Tsix transcription in blocking Xist RNA accumulation but not in X-chromosome choice. *Proc Natl Acad Sci USA* **98:** 10232–10237

Stoker NG, Fairweather NF, Spratt BG (1982) Versatile low-copy-number plasmid vectors for cloning in *Escherichia coli*. *Gene* **18:** 335–341

Turner BM (2002) Cellular memory and the histone code. *Cell* **111:** 285–291

Volpe TA, Kidner C, Hall IM, Teng G, Grewal SI, Martienssen RA (2002) Regulation of heterochromatic silencing and histone H3 lysine-9 methylation by RNAi. *Science* **297:** 1833–1837

Yan Q, Huang J, Fan T, Zhu H, Muegge K (2003) Lsh, a modulator of CpG methylation, is crucial for normal histone methylation. *EMBO J* **22:** 5154–5162